FEM MODELING OF CONCRETE COVER DEGRADATION CAUSED BY REBARS CORROSION IN REINFORCED CONCRETE

Tomasz KRYKOWSKI [a], Adam ZYBURA [b]

[a] Dr.; Faculty of Civil Engineering, The Silesian University of Technology, Akademicka 5, 44-100 Gliwice, Poland
  E-mail address: *Tomasz.Krykowski@polsl.pl*

[b] Prof., Faculty of Civil Engineering, The Silesian University of Technology, Akademicka 5, 44-100 Gliwice, Poland

Abstract

The paper presents an electrochemical description of rebar corrosion and a method of numerical analysis of concrete cover degradation resulting from corrosion. The paper presents formulation of strain state in the concrete cover, caused by corrosion products. The formulation is based on the plasticity theory with distortion, and an incremental formulation of the problem that allows for computational implementation. The distortional strain tensor is a function of an electric current density. A numerical example of determination of a concrete cover splitting time is included.

Streszczenie

W pracy przedstawiono elektrochemiczny opis korozji zbrojenia oraz sposób analizy numerycznej wywołanej tym procesem degradacji otuliny betonowej konstrukcji żelbetowych. Przedstawiono koncepcję określenia stanu odkształcenia w otulinie, wywołanego produktami reakcji na podstawie teorii plastyczności z dystorsjami oraz przyrostowe sformułowanie zagadnienia, pozwalające na implementację algorytmu obliczeniowego. Tensor dystorsyjnych odkształceń korozyjnych opisano jako funkcję gęstości prądu. Przeanalizowano przykład numeryczny wyznaczania czasu odspojenia otuliny betonowej.

1. INTRODUCTION

Reinforced structure corrosion is most often signalized by concrete cover damage – scratches, longitudinal fractures and rust seepage from such fractures. The phenomena observed on the concrete surface result from a two-phase process. In the second phase the developing rebar corrosion causes reactions between other components subsequently created which, by increasing their volume, generate stress in concrete. After reaching the tensile stress limit the separation of concrete cover occurs.

The past written papers have treated the problem of cover damage in an analytical way on the basis of durability solutions, [1, 2, 3]. Computer models have more powerful capabilities for the detailed monitoring of degradation progress resulting from environmental influences, [4, 5].

The aim of this paper is formulation of FEM model that allows for a numerical analysis and prediction of concrete cover splitting time. The paper presents the numerical implementation of the model of corrosion that is based on the transition zone increase concept [5]. The presented method of analysis and in particular the connection of electrochemical and mechanical solutions is new in the analysis of corrosion problems.

2. ELECTROCHEMICAL DESCRIPTION OF CONCRETE COVER CORROSION

2.1. Conditions of rebar corrosion

In the initial service time of reinforced concrete structures rebars are protected against corrosion as a result of the influence of the liquid phase of the concrete cover. The highly alkaline ($pH \approx 12.5 \div 5$) water

solution absorbed by the pores of the walls causes the reinforcing steel surface to be coated by an oxide layer and thus so-called passive state occurs – Fig. 1.
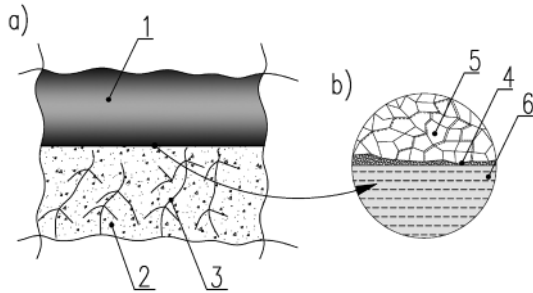
Figure 1.
The rebar-concrete contact: a) macro level, b) micro level; 1 – steel, 2 – concrete cover, 3 – pore structure with the adsorbed moisture, 4 – pasive oxide layer, 5 – steel grain structure, 6 – alkaline pore solution with pH≥12.5

The carbon dioxide diffusion from the atmosphere results in concrete cover carbonatization and in decreasing of the pore solution alkalinity, initially in the concrete surface zones, then with the passage of time in deeper regions. The chloride that can be found in the concrete structure surroundings and which is a strong depassivater, can often migrate as well into the concrete cover. The presence of aggressive factors at a distance from the rebar surface does not violate the passive state – Fig. 2a, however, reaching the rebar's surface by these compounds can result in the loss of concrete capabilities to protect the rebar from corrosion and the reinforcement corrosion process can be initiated – Fig. 2b.
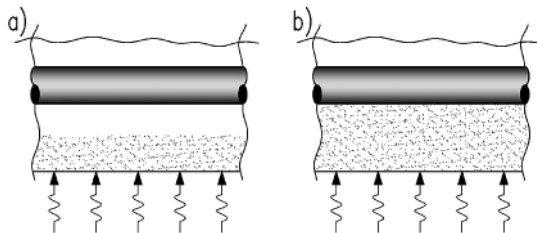
Figure 2.
Concrete cover protection capability losing range: a) corrosion protected, b) corrosion endangered

The progress of concrete carbonization and chloride migration is described in the literature, cf. [6, 7, 8, 9, 10]. In the situation where in the close neighbourhood of the rebar the concrete carbonization process decreases the *pH* factor to *pH ≤ 11.8*, decomposition

of the passive layer and the growth of steel corrosion begins [11]. It is assumed in case of chloride diffusion that the risk of corrosion exists when the chloride concentration reaches 0.4% of the cement mass [11].

The passive layer decomposition initiates reinforcement corrosion, that is an electrochemical process described by the equations

$$2Fe \rightarrow 2Fe^{2+} + 4e^- \tag{1}$$

$$O_2 + 2H_2O + 4e^- \rightarrow 4OH^- \tag{2}$$

$$\overline{2Fe + O_2 + 2H_2O \rightarrow 2Fe^{2+} + 4OH^-}. \tag{3}$$
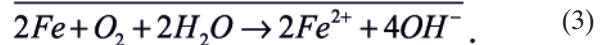
Anode reaction (1) and cathode reaction (2) occur at the same time. As a result of anode reaction (1) the dissolving of iron (in steel) and transition into an ion state takes place. The electrons that are created in the anode reaction (1) are consumed in the cathode reaction (2).

2.2. Steel – solution ion flow through the boundary

In the anode reaction (1) the ions move out from the steel's crystalline structure and go through the phase border into the solution. Similarly the hydrated ferrous ions are transferred in the inverse direction through the phase boundary from the solution – Fig. 3.
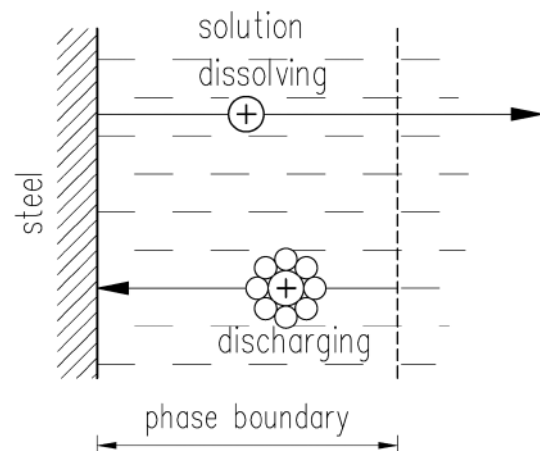
Figure 3.
The scheme of ferrous ions flowing through the phase boundary reinforcing steel-pore solution

Along with the ions the electric charges are transferred through the phase border creating a ferrous (steel) dissolution current with $i_\rightarrow$ density and discharge current with $i_\leftarrow$ density. The resultant current accompanying the anodic reaction (1) is equal to the difference

$$i = \overrightarrow{i} - \overleftarrow{i}. \qquad (4)$$

In the situation where the electrode reaction (1) does not occur, there is no effective current flow $i = 0$. However, the ion transfer in the double layer boundaries results in the exchange current $i_0 = \overrightarrow{i} = \overleftarrow{i}$.

The current flow through the phase border $(i > 0)$ results in electrolytic polarization whose potential takes the value

$$E_i = E + \eta \qquad (5)$$

where E is a potential in the equilibrium state, η overpotential, that is the potential difference between the polarized electrode, the result of current flow density i, and analogous electrode in the current outflow situation. Depending on the dominant type of electrode mechanism there can be activation η_a, concentration η_c and ohm η_o overpotential.

The galvanic potential E_a of the anode reaction (1) and E_c of the cathode reaction (2) in the outflow situation can be approximated by using Nernst equation [10, 11]

$$E_a = E_a^0 + \frac{RT}{2F} \ln\left[Fe^{2+} \right], \qquad (6)$$

$$E_c \cong E_c^0 + 2{,}303 \frac{RT}{F} \left(14 - pH\right), \qquad (7)$$

where E_a^0 and E_c^0 are standard potentials in the equilibrium anode and cathode reaction, $[Fe^{2+}]$ is mole concentration of ferrous ions, R – universal gas constant, T – absolute temperature and K – a chemical equilibrium constant. These potentials have been described with respect to the reference standard hydrogen electrode that takes the zero value.

The activation overpotential of anode reaction is [10, 11]

$$\eta_a = \eta = -\frac{RT}{2\alpha F} \ln i_0 + \frac{RT}{2\alpha F} \ln i. \qquad (8)$$

where α is a coefficient of electrode reaction transition. The concentration overvoltage in cathode reaction can be described by the formula [10, 11]

$$\eta_c = \eta = \frac{RT}{F} \ln\left(1 - \frac{i}{i_{\lim}}\right). \qquad (9)$$

where i_{lim} is limit density of cathode electric current.

2.3 Corrosion process intensity

Because of the fact that corrosion process results from the parallel existence of two reactions (1) and (2), the corrosion process potential E_{corr} results from mixed potential of anode and cathode reaction $E_{corr} = E_{ia} = E_{ic}$, where E_{ia}, E_{ic} are potential of anode and cathode reaction while current flows. According to the mixed potentials theory the density of electric current that is a measure of corrosion rate can be described graphically by the Evans diagram. If the activation polarization decides on the corrosion rate in case of the anodic reaction and the concentration polarization in the cathode reaction case, the Evans diagram has the form presented in Fig. 4.
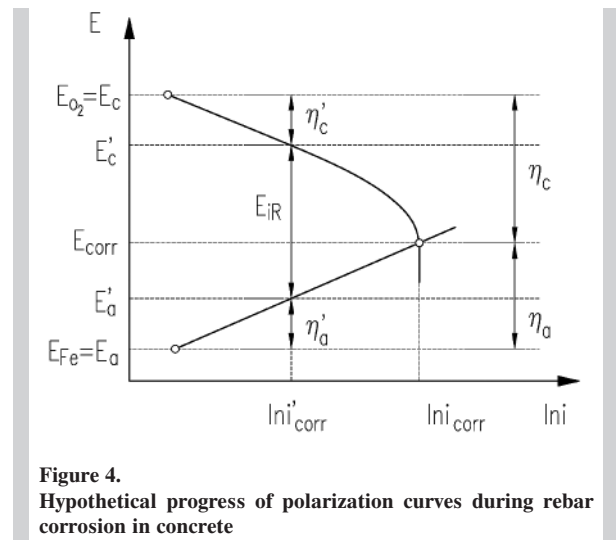
Figure 4.
Hypothetical progress of polarization curves during rebar corrosion in concrete

If steel does not corrode, and remains in invertible ion equilibrium, additionally the density of exchange current is $i_{0,Fe}$, the equilibrium potential of anode reaction takes the value $E_{Fe} = E_a$. Simultaneously, if the steel is oxygenated in the inverse exchange process with the hydroxyl ions, the cathode reaction equilibrium potential at the density of exchange current i_{0,O_2} is $E_{O_2} = E_c$

The existing polarization in the process of corrosion makes the anode and cathode reaction potentials approach each other. In the situation where there is a contact of reinforcement and pore solution, for the corrosion products breaking the process of corrosion the following formula is obtained according to the Evans diagram

$$\ln i'_{corr} = \frac{(E_c - E_a) - \left(\eta'_c + \eta'_a\right)}{\sum_i R_i}, \qquad (10)$$

where $\sum_i R_i$ means the sum of electrical resistance in the corroding system, E_{iR} – the potential drop as the result of this resistance. If the electrical resistance of the corrosion system is not important $\sum_i R_i \to 0$ the potential difference $E'_c - E'_a \to 0$ and the anode and cathode potentials will almost equalize, finally giving the values of corrosion potential E_{corr} and correspondent corrosion current density $\ln i_{corr}$.

According to Faraday's law the transfer rate of ferrous ions into the pore solution can be described by the formula

$$\dot{m} = \frac{dm}{dt} = kI(t) = \gamma_{Fe}\dot{V}, \quad I = i_{corr}A, \quad (11)$$

where: t is time, k – electrochemical equivalent of iron, I – corrosion electric current intensity as a function of time, $\dot{m}$ – transfer rate of ferrous ions into the pore solution, $\dot{V}$ – rate of reinforcement corrosion cavity volume change with surface A, γ_{Fe} – density of iron.

It is possible to assume that the ratio of the mass of corrosion products m_p that are produced on the rebar's surface to the mass of ferrous ions is a constant quantity [5],

$$\frac{m_p}{m} = \frac{\gamma_p}{\gamma_{Fe}}\frac{V_p}{V} = \alpha, \quad \frac{\gamma_p}{\gamma_{Fe}}\beta = \alpha, \quad \beta = \frac{V_p}{V} \quad (12)$$

where: V_p denotes corrosion product volume, γ_p – corrosion product density, α – proportionality coefficient of corrosion products mass to the mass of ferrous ions that are transferred into the solution, and β – proportionality coefficient of corrosion products volume to the corrosion reinforcement cavity.

Differentiating equation (12) the formulas describing the rate of corrosion mass product and the rate of corrosion product volume change as a function of electric current intensity are obtained [5]

$$\dot{m}_p = \alpha\dot{m} = \alpha kI_{corr}, \quad \dot{V}^p = \frac{\alpha}{\gamma_p}kI_{corr} = \frac{\beta}{\gamma_{Fe}}kI_{corr}. \quad (13)$$

3. STRONG FORMULATION OF REINFORCED CONCRETE DEGRADATION MODEL

A two component model $B \subset R^3$ will be considered – a skeleton with chloride ions or carbon dioxide diffusing in pores where the influence of ions Cl^- and CO_2 on the momentum balance of the body is negligibly small. The isothermal character of the thermo-mechanical process and small strain hypothesis for the skeleton $\Omega = \varphi(B) \cong B$ will be assumed, φ is a motion function, Ω – location of the body B in the current configuration, ∂B boundary of the body. On the boundary $\partial B = \Gamma_u \cup \Gamma_\sigma \cup \Gamma_c \cup \Gamma_j$ the parts of boundary $\Gamma_u, \Gamma_\sigma, \Gamma_c, \Gamma_j$ where the displacement vector, traction vector, concentration and mass flux of chloride ions or carbon dioxide are distinguished. The strong formulation of the problem can be presented by a system of differential equations describing the boundary value problem of mass transport and momentum balance equations [7, 12]:

• mass transport of aggressive substance migrating in the concrete pores

$$\left.\begin{array}{l} \dot{c} + \text{div}\,\mathbf{j} = 0, \quad \mathbf{j} = -k\,\text{grad}\,c, \\ \mathbf{j} = \mathbf{j}(\mathbf{x},t), \quad c = c(\mathbf{x},t) \end{array}\right\} \mathbf{x} \in \mathbf{B}, \quad t \in [0,T],$$
$$c = \bar{c}, \quad \mathbf{x} \in \Gamma_c; \quad \mathbf{j}\cdot\mathbf{n} = -\bar{j}, \quad \mathbf{x} \in \Gamma_j, \quad t \in [0,T]. \quad (14)$$

where $\mathbf{x}$ is particle location in the deformed configuration, $c = c(\mathbf{x},t)$ – aggressive substance mass concentration, $\mathbf{j}$ – aggressive substance mass flux, $\mathbf{n}$ – normal vector.

• momentum balance

$$\left.\begin{array}{l} \text{div}\,\sigma + \rho\mathbf{b} = 0, \quad \sigma = \mathbf{C}:\varepsilon^e, \quad \varepsilon^e = \varepsilon - \varepsilon^p - \varepsilon^d, \\ \varepsilon = \text{grad}^s\mathbf{u} = \frac{1}{2}(\text{grad}\,\mathbf{u} + \text{grad}^T\mathbf{u}), \quad \mathbf{u} = \mathbf{u}(\mathbf{x},t); \end{array}\right\} \mathbf{x} \in \mathbf{B},$$
$$\mathbf{u} = \bar{\mathbf{u}}, \quad \mathbf{x} \in \Gamma_u, \quad \sigma\cdot\mathbf{n} = \mathbf{p}, \quad \mathbf{x} \in \Gamma_t, \quad t \in [0,T]. \quad (15)$$

where σ is stress tensor, $\mathbf{b}$ – mass force vector, $\mathbf{C}$ – elasticity tensor, $\mathbf{u}$ – vector of particle displacement, ε – infinitesimal strain tensor, ε^e – elastic strain tensor, ε^p – plastic strain tensor, ε^d – distortional strain tensor resulting from volumetric increase of corrosion products and $\mathbf{p}$ – traction force vector.

4. APPLICATION OF ELASTO-PLASTIC MEDIA THEORY

The mechanical processes related to the corrosion product formed on the rebar's surface have an influence on the state of stress in the concrete cover and

are described using the plasticity theory without hardening. The elastic-plastic equations with distortions have the following form [13]:

• constitutive relationships

$$\boldsymbol{\sigma} = \mathbf{C} : \varepsilon^e = \mathbf{C} : (\varepsilon - \varepsilon^p - \varepsilon^d) = \mathbf{C} : (\varepsilon^{ed} - \varepsilon^p),$$
$$\varepsilon = \varepsilon^e + \varepsilon^p + \varepsilon^d, \quad \varepsilon^{ed} = \varepsilon - \varepsilon^d, \quad \varepsilon^d = \varepsilon^d(I_{corr}), \tag{16}$$

• continuum elastic-plastic tangent stiffness tensor of the material, [13]

$$\dot{\boldsymbol{\sigma}} = \mathbf{C}^{ep} : (\dot{\varepsilon} - \dot{\varepsilon}^d) = \mathbf{C}^{ep} : \dot{\varepsilon}^{ed}, \quad \mathbf{C}^{ep} = \mathbf{C} - \frac{1}{h}\mathbf{m} \otimes \mathbf{m}, \tag{17}$$

$$\mathbf{m} = \mathbf{C} : \frac{\partial f}{\partial \boldsymbol{\sigma}}, \quad h = \frac{\partial f}{\partial \boldsymbol{\sigma}} : \mathbf{C} : \frac{\partial f}{\partial \boldsymbol{\sigma}}, \quad \dot{\varepsilon} = \dot{\varepsilon}^e + \dot{\varepsilon}^p + \dot{\varepsilon}^d, \quad \dot{\varepsilon}^p = \dot{\gamma}\frac{\partial f}{\partial \boldsymbol{\sigma}}.$$

In equations (16, 17) C^{ep} – continuum elastic–plastic tangent stiffness tensor, $\dot{\gamma}$ – magnitude of plastic strains, f – flow surface.

5. STATE OF STRESS AND STRAIN IN THE COVER

5.1. Concept of transition zone increase

The concrete cover degradation process that is a result of corrosion product increase is described by the transition zone that can be modified over time. The concept of transition zone was signalized in paper [5]. The real system composed of concrete, reinforcement and corrosion product is modeled by a medium where additionally a transition layer around the rebar is taken into consideration. The corrosion products are produced locally in the electric cell initiation places. The intensity of these processes changes depending on the point on the outer surface of the rebar that is considered. The intensity of the process changes is also related to the variation over time in the chloride ion concentration in the cover and to the location of the carbonization front. The macroscopic effect of electrochemical process results in corrosion product creation that occurs in the transition zone in the characteristic crescent form.

It needs to be taken into consideration that the cover degradation phenomenon requires formulation of a dependence that allows for the local description of volume product changes in the finite element as a function of electric current intensity or density. One of the methods allowing for the local formulation of corrosion product growth is the approach that assumes distortional strains that are a function of electric current intensity increase in the transition zone. The linking of this concept with the approximation of finite elements permits formulation of corrosion product growth effect

on the state of stress in the cover which is analogical to the local thermal strain effect. The major assumption of the estimation method for assessing the corrosion influence on the stresses state in the cover can be presented in the form of three postulates [5]:

• The corrosion cell on the rebar surface area is created after having reached favourable conditions for the electrode process.

• The volumetric increase of finite elements in the transition zone concerns only such elements that are located in the neighbourhood of the electrochemical process initiation point.

• In case when a larger number of finite elements take part in the process, the corrosion product mass increase accruing in the finite elements is divided proportionally to the number of active finite elements.

A model of transformations occurring in the concrete and in the cover as a result of active environmental factors is presented in Fig. 5.
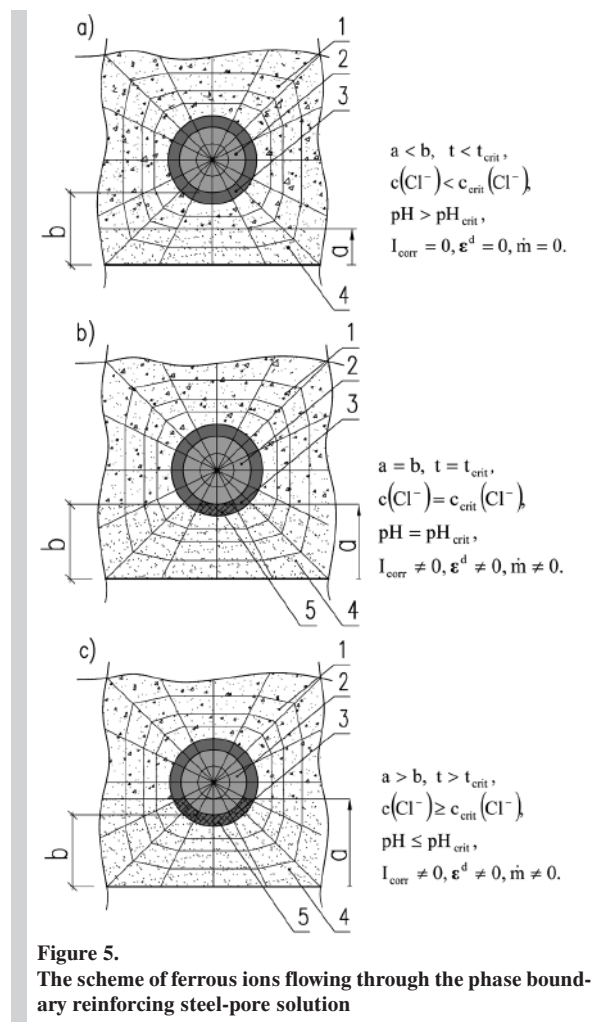
Figure 5.
The scheme of ferrous ions flowing through the phase boundary reinforcing steel-pore solution

In the situation when zone *4*, with a range of decreasing protection properties of concrete $c(Cl^-) < c_{crit}(Cl^-)$, $pH > pH_{crit}$, is smaller than the thickness b of the cover, the reinforcement is not corroding $I_{corr} = 0$, $\dot{m} = 0$, distortional strain is not present $\dot{\varepsilon}^d = 0$ and the elements of the transition layer *3* are passive – Fig. 5a.

After matching the range of decreasing protection properties of concrete with the cover thickness ($a = b$) the initiation of reinforcement corrosion follows $I_{corr} \neq 0$, $\dot{m} \neq 0$ and the distortional strain $\dot{\varepsilon}^d \neq 0$ that is modeling by the transition layer *3* in sector *5* (Fig. 5b) grows. Further progress in the range $a > b$ causes an extension of the zone of active elements *3* (Fig. 5c).

5.2. Formulation of substitute corrosion material expansion coefficient

The parameter that is determined here is the distortional strain tensor in the transition layer. Its components are functions of the electric current intensity. Assuming small strains the following assumption can be formulated, [14]

$$I_{\varepsilon^d} = \frac{V(t) - V_0}{V_0} \equiv \frac{V^d(t) - V_0}{V_0} \cong \mathbf{tr}\left(\varepsilon^d\right). \quad (18)$$

It can be assumed when modeling the corrosion problem that the mass production occurs only in directions perpendicular to the rebar axis. Assuming that the rebar axis determines local X_3 direction the assumptions that $\varepsilon^d_{33} = 0$ and $\varepsilon^d_{11} = \varepsilon^d_{22} = \varepsilon$ are made. After differentiating equation (18) with respect to time, the definition of distortional strain tensor as a function of electric current intensity is obtained:

$$\dot{\varepsilon}^d = \tilde{\mathbf{1}} \frac{\beta k}{2 V_0 \gamma_{Fe}} I_{corr}(t), \qquad \tilde{\mathbf{1}} = \begin{cases} \delta_{ij} \mathbf{e}_i \otimes \mathbf{e}_j \ for \ i,j \neq 3 \\ \mathbf{0} \ other \ situation \end{cases} \quad (19)$$

In equation (19) $\boldsymbol{\varepsilon}^d$ is distortional strain created by corrosion products at the steel – concrete contact, δ_{ij} – Kronecker delta.

6. INCREMENTAL FORMULATION OF REINFORCED CONCRETE DEGRADATION PROBLEM

The solution of concrete cover degradation problem using FEM requires the replacement of the strong formulation of the problem, defined by equations (14), (15), by a weak formulation. By using the Eulers backward integration scheme the weak form of mass balance equation describing transport of aggressive media in the body B at time t_{n+1} can be formulated in the form

$$W(c_{n+1}, \delta c) = \int_B \delta c \cdot (c_{n+1} - c_n) dB - \Delta t \int_B [grad \delta c \cdot \mathbf{j}]_{n+1} dB - \Delta t \int_{\partial B} [\delta c \cdot \bar{j}]_{n+1} d\partial B = 0. \quad (20)$$

The time independent weak form of momentum balance equation can be written directly at time t_{n+1} in the form

$$G(\mathbf{u}_{n+1}, \varepsilon^d_{n+1}, \delta \mathbf{u}) = \int_B \varepsilon(\delta \mathbf{u}) : \sigma_{n+1} dB - \int_B \delta \mathbf{u} \cdot \rho \mathbf{b}_{n+1} dB - \int_{\partial B} \delta \mathbf{u} \cdot \mathbf{p}_{n+1} d\partial B = 0. \quad (21)$$

In equations (20), (21) $\delta \mathbf{u}$ is variation of displacement field, δc variation of concentration field and the indexes n+1 and refer to time moments t_{n+1} and (where $t_{n+1} = t_n + \Delta t_{n+1}$), respectively. The constitutive relationships defining the stress tensor σ_{n+1} at time t_{n+1} in equation (21) can be defined using Euler backward rule in (17) in the form

$$\sigma_{n+1} = \sigma_n + \mathbf{C}^{ep} : \Delta \varepsilon^{ed}_{n+1}, \quad \Delta \varepsilon^{ed}_{n+1} = \Delta t_{n+1} \dot{\varepsilon}^{ed}(t_{n+1}), \quad \varepsilon^{ed}_{n+1} = \varepsilon_{n+1} - \varepsilon^d_{n+1} \quad (22)$$

The solution of equation (21) requires the application of the Newton-Raphson method. The iteration process can be constructed by linearization of (21) in the neighborhood of points $\mathbf{u}^k_{n+1}$ and I^k_{n+1} [13]

$$G = \bar{G} + D\bar{G} \cdot \Delta \mathbf{u}^{k+1}_{n+1} + D\bar{G} \cdot \Delta I^{k+1}_{n+1}, \quad G = G(\mathbf{u}^{k+1}_{n+1}, I^{k+1}_{n+1}, \delta \mathbf{u}), \quad \bar{G} = \bar{G}(\mathbf{u}^k_{n+1}, I^k_{n+1}, \delta \mathbf{u}),$$
$$\mathbf{u}^{k+1}_{n+1} = \mathbf{u}^k_{n+1} + d\Delta \mathbf{u}^{k+1}_{n+1}, \quad I^{k+1}_{n+1} = I^k_{n+1} + d\Delta I^{k+1}_{n+1}, \quad t^{k+1}_{n+1} = t^k_{n+1} + d\Delta t^{k+1}_{n+1}, \quad (23)$$
$$DG(\mathbf{x}) \cdot \mathbf{u} = \left. \frac{d}{d\alpha} \right|_{\alpha=0} G(\bar{\mathbf{x}} + \alpha \mathbf{u}), \quad \mathbf{x} = \bar{\mathbf{x}} + \alpha \mathbf{u}.$$

Index k refers to subincrement number of internal correction arguments at time interval $\langle t_n, t_{n+1} \rangle$. As the result of linearization the incremental equation allowing for elastic-plastic analysis of structure with mechanical distortions resulting from corrosion products creation is obtained. The additional term in (23) in comparison with the standard elastic plastic analysis is the one describing the influence of electric current intensity on the rate of distortional strain creation

$$D\bar{G} \cdot \Delta I^{k+1}_{n+1} = \int_B \varepsilon(\delta \mathbf{u}) : \left[\frac{\partial \sigma}{\partial \varepsilon^d} \right]^k_{n+1} : d\Delta \varepsilon^{dk+1}_{n+1} dB, \quad d\Delta \varepsilon^{dk+1}_{n+1} = \left[\frac{\partial \varepsilon^d}{\partial I} \right]^k_{n+1} \cdot d\Delta I^{k+1}_{n+1},$$
$$\left[\frac{\partial \varepsilon^d}{\partial I} \right]^k_{n+1} = \left[\frac{\partial \sigma(\mathbf{u}^k_{n+1}, I^k_{n+1} + \alpha d\Delta I^{k+1}_{n+1}, \delta \mathbf{u})}{\partial \varepsilon^d(I^k_{n+1} + \alpha d\Delta I^{k+1}_{n+1})} : \frac{\partial \varepsilon^d(I^k_{n+1} + \alpha d\Delta I^{k+1}_{n+1})}{\partial (I^k_{n+1} + \alpha d\Delta I^{k+1}_{n+1})} \cdot \frac{\partial(I^k_{n+1} + \alpha d\Delta I^{k+1}_{n+1})}{\partial \alpha} \right]_{\alpha=0} \quad (24)$$

The computational algorithm can be presented in the following form:

• Computation of aggressive media concentration field.

The computation of aggressive substance concentration field distribution by the use of equation (20) must be done. If in the time interval $t \in \langle t_n, t_{n+1} \rangle$ the favorable condition for corrosion is reached, the

process of rust production will be activated.
- Computation of distortional strain increment as the result of corrosion products creation.

The distortional strain increment $d\Delta\varepsilon^{dk+1}_{n+1}$ is a function of time varying corrosion current intensity. We can assume that the time increment $d\Delta t^{k+1}_{n+1} \in \langle t_n, t_{n+1}\rangle$ in the time interval $\langle t_n, t_{n+1}\rangle$ is described by the function

$$t^{k+1}_{n+1} = t^k_{n+1} + d\Delta t^{k+1}_{n+1}, \quad t^0_{n+1} = t_n, \quad d\Delta t^{k+1}_{n+1} = \frac{t_{n+1} - t^k_{n+1}}{N} \quad (25)$$

where in equation (25) N is a natural number. Using backward Euler's scheme in eq. (19) the distortional strain increment can be formulated in the time interval $d\Delta t^{k+1}_{n+1} = t^{k+1}_{n+1} - t^k_{n+1}$ in the form

$$d\Delta\varepsilon^{dk+1}_{n+1} = \varepsilon^{dk+1}_{n+1} - \varepsilon^{dk}_{n+1} = \tilde{\mathbf{1}}\frac{\beta k}{2V_0\gamma_{Fe}}d\Delta t^{k+1}_{n+1}I_{corr}\left(t^{k+1}_{n+1}\right), \quad (26)$$

$$\varepsilon^{dk+1}_{n+1} = \varepsilon^{dk}_{n+1} + \Delta\varepsilon^{dk+1}_{n+1}, \quad \varepsilon^{d0}_{n+1} = \varepsilon^d_n.$$

- Displacement field computation.

Making use of equations (22-24) the linearized momentum balance equation where $d\Delta\varepsilon^{dk+1}_{n+1}$ s defined by (26) can be presented in the form

$$\int_B \varepsilon(\delta\mathbf{u}):\mathbf{C}^{ep}\Big|^k_{n+1}:d\Delta^{k+1}_{n+1}dB - \int_B \varepsilon(\delta\mathbf{u}):\mathbf{C}^{ep}\Big|^k_{n+1}:d\Delta\varepsilon^{dk+1}_{n+1}dB = F^{ext}_{n+1} - F^{intk}_{n+1}, \quad (27)$$

$$F^{ext}_{n+1} = \int_B \delta\mathbf{u}\cdot\rho\mathbf{b}_{n+1}dB + \int_B \delta\mathbf{u}\cdot\mathbf{p}_{n+1}dB, \quad F^{intk}_{n+1} = \int_B \delta\varepsilon:\sigma^k_{n+1}dB, \quad (28)$$

$$\mathbf{C}^{ep}\Big|^k_{n+1} = \frac{\partial\sigma}{\partial\varepsilon}\Big|^k_{n+1} = -\frac{\partial\sigma}{\partial\varepsilon^d}\Big|^k_{n+1}, \quad \mathbf{u}^{k+1}_{n+1} = \mathbf{u}^k_{n+1} + d\Delta\mathbf{u}^{k+1}_{n+1}, \quad \mathbf{u}^0_{n+1} = \mathbf{u}_n, \quad (29)$$

- Convergence criteria.

The condition for obtaining convergence at time increment $\Delta t_{n+1} = t_{n+1} - t_n$ is presented in the form

$$\frac{\|\mathbf{u}^{k+1}_{n+1} - \mathbf{u}^k_{n+1}\|}{\|\mathbf{u}^k_{n+1}\|} \le TOL_1, \quad \frac{\|t_{n+1} - t^k_{n+1}\|}{\|t^k_{n+1}\|} \le TOL_2. \quad (30)$$

The condition (30.2) informs us about reaching the time t_{n+1} at the end of time step.

7. NUMERICAL ANALYSIS

The theoretical considerations have been verified by a numerical analysis carried out using a system for FEM analysis. The analysis is made by using separated parts of a reinforced concrete element that contain rebar with diameter $\phi_0 = 20$ and 40 mm thick concrete cover, Fig. 6.

The computational model is 100x100x10 mm part, virtually cut from the structure, containing a rebar ideally connected with the concrete. The division into
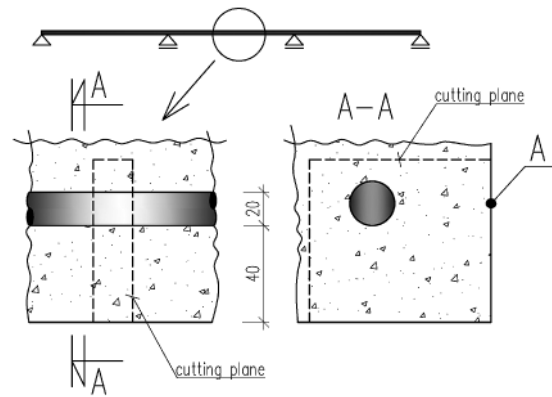
Figure 6.
Analyzed numerical example
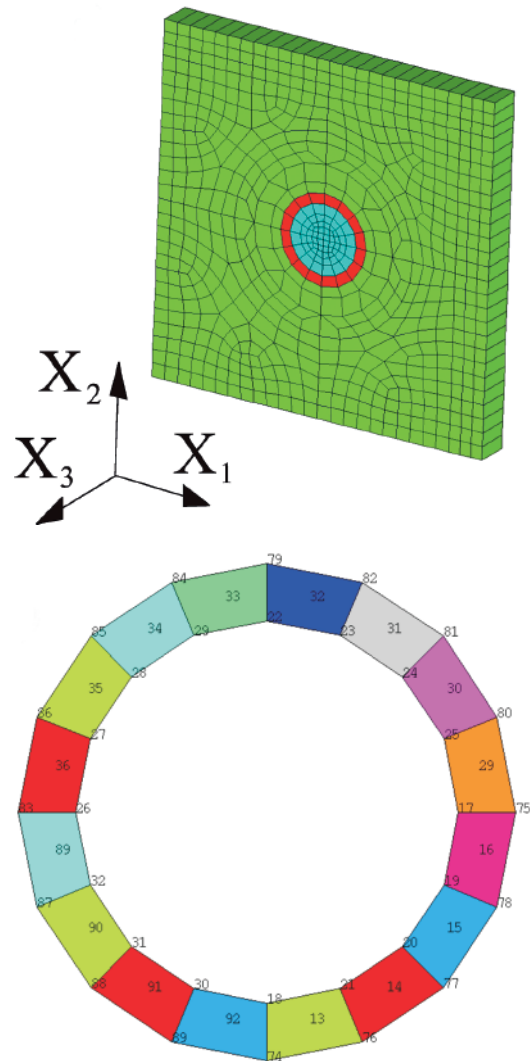
Figure 7.
Finite element mesh a) in the entire model, b) in the ring of active finite elements surrounding reinforcement (node and element numbers shown)

solid 8-node finite elements is assumed. The finite element model along with the detailed finite element mesh is visualized in Fig. 7. It has been assumed that the virtually cut part of the structure satisfies plain strain conditions. It has also been assumed that for nodes lying in the cutting plain displacements in normal directions are fixed.

Because there was no possibility of interfering in the finite element code the analysis has been simplified and performed in two parts. The chloride ions transfer analysis is performed in the first stage. In the second stage the mechanical elastic-plastic analysis with the distortions that are produced as a result of the rebar corrosion process is performed. The distortional loading in the simplified analysis is applied at the end of time step t_{n+1}.

The target of the numerical analysis of chloride ions transfer inside the concrete is determination of time after which the critical concentration $C_{crit} = 0.4\%$ in the finite element nodes that are located in the active ring of transition zone is reached. In the numerical analysis of chloride ions diffusion inside a concrete structure (concrete C25/30 with diffusion coefficient $k = 2 \cdot 10^{-8}$ cm²/s) is assumed [7]. The concentration change diagrams at the nodes located on the steel-concrete contact surface and time after which chloride ions concentration exceeds the critical concentration C_{crit} has been obtained, cf. Fig. 8. It can be stated on the basis of node concentration changes that at time interval $\tau = t - t_{crit}$ the following finite elements are activated: t=0, elements number 13, 14, 15, 16; t=2, elements number 92, 29; t=4, elements number 91, 30; t=6, elements number 90, 31; t=7, elements number 89, 32.
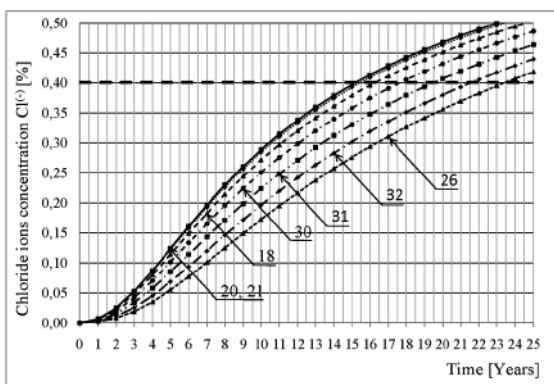
Figure 8.
Concentration change of chloride ions in nodes of the transition zone steel–concrete; the numbers on the curves refers to numbers of FEM nodes

For the assumed concrete B25/30 according to [7, 21] the mean value of compressive strength is $f_{cm} = 33$ MPa, the mean value of tensile strength is $f_{ctm} = 33$ MPa , elasticity modulus is $E_{cm} = 31$ GPa . The Drucker-Prager plasticity model is used to describe concrete. The required input data have been calculated using the following formulas [17].

$$\alpha = \frac{m-1}{\sqrt{3}\cdot(m+1)}, \quad k = \frac{2\cdot\sigma_c}{\sqrt{3}\cdot(m+1)}, \quad m = \frac{\sigma_c}{\sigma_t} = \frac{f_{cm}}{f_{ctm}},$$
$$c = \frac{\sqrt{3}\cdot k\cdot(3-\sin\varphi)}{6\cdot\cos\varphi}, \quad \varphi = \arcsin\left(\frac{3\sqrt{3}\cdot\alpha}{\sqrt{3}\cdot\alpha+2}\right). \tag{31}$$

According to these formulas the cohesion coefficient is $c = 4.33 \cdot 10^6\ N/m$, the angle of internal friction is equal to $\Phi = 60.57$. The reinforcing steel A-I is used with the elastic material model. Based on [15, 16] the elasticity module $E_s = 200$ GPa is accepted. The corrosion electric current density i is determined on the basis of the empirical equation presented in paper [15]:

$$\ln(1.08i) = 7.89 + 0.771\cdot\ln(1.69Cl) - 3006\frac{1}{T} - \frac{1.16}{10^4}R_c + 2.24t^{-0.215} \tag{32}$$

where i is corrosion electric current density [$\mu A/cm^2$], Cl – chloride ions content in concrete [kg/m], T – steel surface temperature [K], R_c – concrete cover electric resistance [Ohm], t – corrosion process time [years].

To determine the corrosion electric current density i, the chloride concentration in concrete $c_{Cl} = 0.4$ [%] of cement mass, cement content in concrete $m_{cem} = 250$ [kg/m^3], rebar surface temperature $t_s = 10$ [°C] and concrete electrical resistance $R_c = 15000$ [Ω] have been assumed.

After electric current intensity function determination

$$I = \pi\varphi\, l_a i \tag{33}$$

where l_a is the length of section of active corrosion processes on the rebar. Taking into consideration the electrochemical equivalent of iron $k = 9.12 \cdot 10^{-3}\ g/\mu A\cdot year$ and ferric density $\gamma_{Fe} = 7.85\ g/cm^3$, the rate of volumetric changes of corrosion products $\dot{V}_p$ that determine the value of the distortional strain has been estimated according to formula (6). Three ratios of corrosion product volume to corrosion cavity volume $\beta = V_p/V$ - $\beta = 2, \beta = 3, \beta = 4$, have been taken into consideration. The results obtained for time changes of corrosion current density functions i and major tension stress S₁ on the element edge (at point A according to Fig. 6) are presented graphically in Fig. 9.
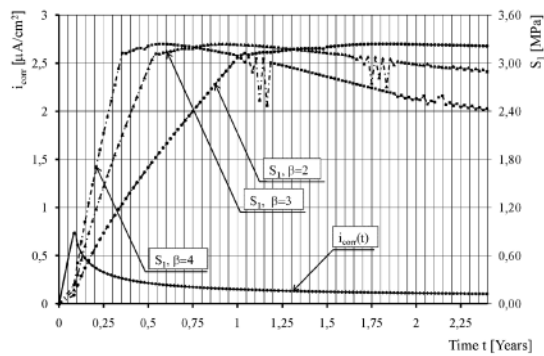
Figure 9.
The results of computer calculations of maximum tension stresses S_1 in the model at point A (cf. Fig. 5) in the function of time and electric current density; description in text

Reaching the stress level S_1, the concrete strength in tension f_{ctm} = 3.3 MPa lasts through the time interval t from the moment of electrochemical process initiation to the fracturing of the concrete cover. This time interval substantially depends on the β parameter. The concrete cover cracking times and stresses at point A are shown in Table 1.

The distribution of equivalent plastic strain around the analyzed reinforcing bar for the model is shown in Fig. 10.

Table 1.
The results of computer calculations performed according to the model of transition zone increase

β	T [Month]	S1 [MPa]
2	22	3.24
3	11	3.24
4	7	3.23
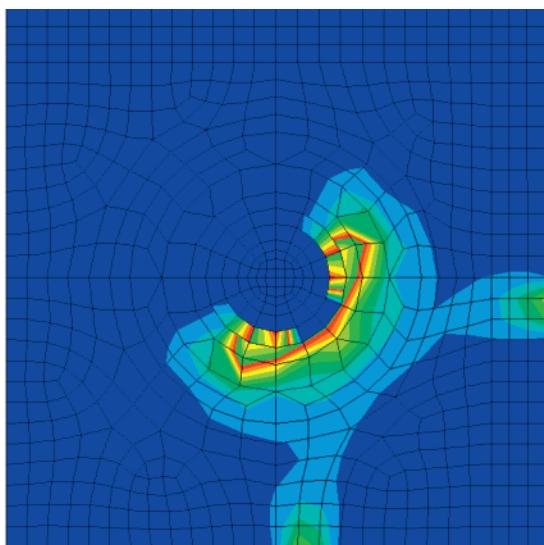
Figure 10.
Equivalent strain distribution around analyzed reinforcing bar at the moment of damage

8. SUMMARY

The paper presents a model allowing for the numerical analysis of concrete cover degradation process. The method deals with the problem of transport of aggressive substances initiating the rebar's corrosion, evolution of a region with active corrosion process and description of mechanical degradation of concrete cover. The linearized weak form of momentum balance equation in respect of displacement and corrosion current intensity increments with mechanical distortions has been shown. Formulating distortional strain tensor, the assumption that the ratio mass of products to mass of ferrous ions transferred into the solution is constant has been made. The algorithm of the analysis of the concrete cover degradation as a function of time has been presented. The numerical example of the phenomenon has been analyzed using the simplified version of the algorithm.

REFERENCES

[1] *Bazant Z. P.*; Physical model for steel corrosion in concrete sea structures – theory. Journal of the Structural Division ASCE, Vol.105, No.6, 1979; p.1137-1153

[2] *Liu T., Weyers R. W.*; Modeling the dynamic corrosion process in chloride contaminated concrete structures. Cement and Concrete Research, Vol.28, No.3, 1998; p.365-379

[3] *Pantazopoulou S. J., Papoulia K. D.*; Modeling cover-cracking due to reinforced corrosion in RC structures. Journal of Engineering Mechanics, Vol.127, No.4, 2001; p.342-351

[4] *Krykowski T.*; Computational model of corrosion damage in the reinforced concrete. Archives of Civil Engineering, Vol. LII, No.2, 2006; p.319-337

[5] *Krykowski T., Zybura A.*; Modeling of corroding rebar interaction with concrete cover. Monography REPROCITY Research and Training on Restoration and Protection of the City Environment in Industrial Regions. Faculty of Civil Engineering, The Silesian University of Technology, Gliwice, 2008.

[6] *Chatterji S.*; On the applicability of Fick's second law to chloride ion migration through portland cement concrete. Cement and Concrete Research, 25, 2, 1995; p.299-303.

[7] *Černý R., Rovnaníková P.*; Transport processes in concrete. London and New York, Spoon – Press, 2002

[8] *Ściślewski Z.*; Ochrona konstrukcji żelbetowych (Protection of reinforced concrete structures). Arkady, Warszawa, 1999 (in Polish)

[9]   *Zybura A.*; Analysis of chloride migration in concrete based on multicomponent medium theory. Archives of Civil Engineering, Vol. 53, No.1, 2007; p.131-150

[10] *Zybura A.*; Degradacja żelbetu w warunkach korozyjnych (Degradation of reinforced concrete in the corrosion conditions). Zeszyty Naukowe Politechniki Śląskiej, Z. 72., Gliwice, 1990 (in Polish)

[11] *Wieczorek G.*; Korozja zbrojenia inicjowana przez chlorki i karbonatyzację otuliny (Rebars corrosion initited by chlorides and concrete cover carbonatization). Dolnośląskie Wydawnictwo Edukacyjne, Wrocław, 2002 (in Polish)

[12] *Wilmanski K.*; Foundations of Phenomenological Thermodynamics. Warsaw, PSP, 1974

[13] *Simo J.C., Hughes T. J. R.*; Computational inelasticity. Springer-Verlag, 1998

[14] *Mase G. T., Mase G. E.*; Continuum mechanics for engineers. Boca Raton – London – New York – Washington D. C, CRC Press, 1999

[15] Comite Euro-International Du Beton.; CEB-FIP model code. Comite Euro-International Du Beton, Switzerland, 1990

[16] Polski Komitet Normalizacyjny.; PN-B-03264:2002. Konstrukcje żelbetowe i sprzężone – Obliczenia statyczne i projektowanie (Plain, reinforced and prestressed concrete structures – Analysis and structural design). Polski Komitet Normalizacyjny, 2002 (in Polish)

[17] *Chen W. F., Zhang H.*; Structural plasticity. Theory problems and CAE software. New York, Springer-Verlag 1990